MODELLING CRATER SHAPES WITH GAUSSIAN RANDOM SPHERES

Tatjana Tchumatchenko[(1) (2)], Karri Muinonen[(3)] , SMART1 AMIE Science Team

[(1)] TU Darmstadt, Institute for Applied Physics, Schlossgartenstr. 7, 64289 Darmstadt, Germany
Email: tatjana.tchumatchenko@physik.tu-darmstadt.de
[(2)] Observatory, P.O. Box 14, FI-00014, University of Helsinki, Finland, Email:tchumat@astro.helsinki.fi
[(3)] Observatory, P.O. Box 14, FI-00014, University of Helsinki, Finland, Email: muinonen@cc.helsinki.fi

ABSTRACT

Impact cratering is an important geological process which affects the majority of the terrestrial planets, moons and asteroids. The size and shape of the craters are determined by the velocity of the impactor and the soil conditions of the target material. The conditions present at the moment of the impact as well as the surface properties can be therefore estimated from the crater shape. Simple crater shapes were modeled so far with hemispheres, or are fitted with polynomials [1]. In this paper we present a novel statistical two-parameter model, which allows both symmetrical and asymmetrical shapes.

1. INTRODUCTION

We take a statistical approach, assuming that each crater is a representation of a Gaussian random hemisphere. This is motivated by the fact that the majority of simple craters on planetary bodies resemble hemispheres. So hemispheres are a good first-order approximation [6], but they do not take into account the irregularities of the craters. We therefore take the hemispheres as a starting point and introduce a Gaussian distortion.

Each shape is unique, but the craters resulting from similar impact events should have similar statistical parameters. We therefore assume that craters which were formed during approximately the same time period in the same region of a planetary body should have similar statistical parameters. In this paper we introduce a way of estimating the statistical parameters of craters from the form of the rim.

We begin this paper by introducing the mathematical formalism of Gaussian random spheres and by showing how it can be used to model crater shapes. We then describe the method we used to extract the rim profile from the nadir viewing images and how the statistical parameters can be estimated from the parameterized rim profile. We then give an outlook on the application of this method to study light scattering inside craters with potential implications for clinometry, and how the crater shapes on different planetary bodies can be statistically compared.

2. GAUSSIAN RANDOM SPHERES

The Gaussian random sphere given by the radial distance $r(\theta,\varphi)$ introduced in [2] and [8] is a lognormally distributed isotropic random field defined on the unit sphere. It can be described by the mean radial distance and the covariance function of the logarithmic radial distance.

$$r(\theta,\varphi) = a \cdot \exp(s(\theta,\varphi) - \frac{1}{2}\beta^2) \qquad (1)$$

$$s(\theta,\varphi) = \sum_{l=0}^{l=\infty} \sum_{m=-l}^{l} s_{lm} Y_{lm}(\theta,\varphi) \qquad (2)$$

The radius as given by Eq. 1 is determined by the spherical harmonics coefficients of the logradius.

The quantity $s(\theta,\varphi)$ is called "logradius" and has zero mean and a standard deviation β. The radius $r(\theta,\varphi)$ has the mean value a and the standard deviation σ determined by the Eq. (3):

$$\sigma = \sqrt{\exp(\beta^2) - 1} \qquad (3)$$

The coefficients s_{lm} of the spherical harmonics Y_{lm} have to fulfill several requirements: Their mean value must be zero and they have to be independent variables with the variances given as by Eq. 5 and Eq. 6:

$$s_{l,-m} = (-1)^m \cdot s_{lm}^{*} \qquad (4)$$

$$Var(\mathrm{Re}(s_{lm})) = (1+\delta_{m0}) \cdot \frac{2\pi}{2l+1} C_l \qquad (5)$$

$$Var(\mathrm{Im}(s_{lm})) = (1-\delta_{m0}) \cdot \frac{2\pi}{2l+1} C_l \qquad (6)$$

δ_{m0} denotes the Kronecker delta function and C_l the Legendre coefficients of the correlation function.
The covariance function for an isotropic random field defined on a unit sphere is given in the Eq. 7:

$$k_s(\gamma) = \beta^2 \cdot C_s(\gamma) = \sum_{l=0}^{\infty} C_l P_l(\cos(\gamma)) \qquad (7)$$

The angle γ is the difference between two solid angles on the unit sphere. The coefficients C_l of the covariance function for the unit sphere have to fulfill the Eq. 8.

$$\sum_{l=0}^{\infty} C_l = \beta^2 \qquad (8)$$

The covariance function for an isotropic random field defined on the unit circle is given in Eq. 9:

$$k_s(\gamma) = \sum_{l=0}^{\infty} \delta_k^2 \cos(k \cdot \gamma) \qquad (9)$$

Starting with the Legendre expansion one can define the correlation angle Γ as

$$\Gamma = 2 \arcsin\left(\frac{1}{2 \cdot \sqrt{(-C_s^{(2)}(0))}} \right) \qquad (10)$$

$C_s^{(2)}(0)$ is the second derivative of the correlation function $C_s(\gamma)$ taken at the position 0.
The correlation angle and the radial standard deviation are important quantities of a random sphere.
For the numerical generation of sample surfaces, one starts with a correlation function $C_s(\gamma)$.

Typically, one chooses $C_s(\gamma)$ to follow a power law or a Gaussian. The correlation function determines the variances of the spherical-harmonics coefficients and allows to calculate the two characteristic quantities σ and Γ. The spherical harmonics coefficients are generated using random variables, which have the variances as defined by the correlation function in Eq. 5 and Eq. 6.

Sample spheres generated by a power law correlation function are shown in Fig. 1. These sample shapes show that lower power-law index weights the spectrum towards higher-degree spherical harmonics and the shapes have more hills per solid angle. The increase in variance enhances the hills radially.

The Gaussian shapes were already used to model the forms of asteroids [2] and in this paper we want to apply this formalism to crater shapes.

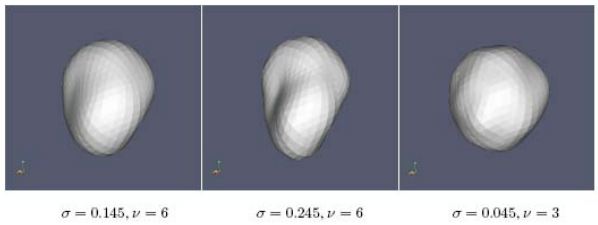

Fig. 1.These sample shapes are generated using a power law correlation function; the standard deviation of radius σ and the power law index ν are given.

3. GAUSSIAN HEMISPHERES

According to [3], the diameter-to-depth ratio of simple lunar craters is 5, therefore we model the craters with a hemisphere which is cut by a plane, in the way that the diameter-to-depth ratio is matched. For lunar craters it corresponds to the height value $z = 0.7241$ for unit sphere. This value fulfills Eq. 11.

$$\left(\frac{2 \cdot \sin(\arccos(z))}{1-z} \right) = 5 \qquad (11)$$

Fig. 2. shows sample crater shapes with the diameter-to-depth ratio =5 which are generated using a power-law correlation function.

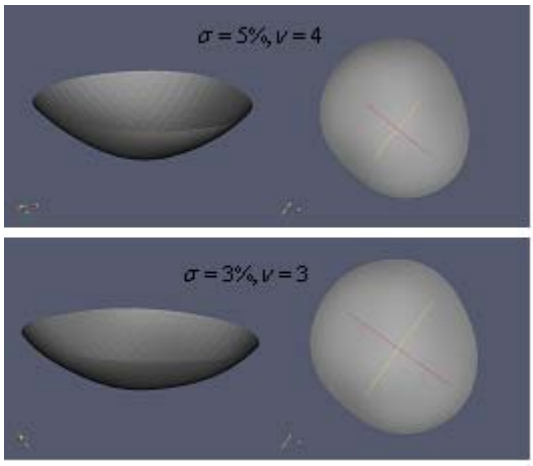

Fig. 2. The nadir view of the sample crater is shown in the right; in the left are the craters as seen from the side. The standard deviation of radius σ and the power-law index ν for each crater are given.

4. RIM PROFILE EXTRACTION

To extract the rim profiles, we used nadir view images and extracted the rim form using active contours.
These are curves that are defined within an image and can move under the influence of internal and external forces. The forces are defined in such a way, that the active contour will conform to an object boundary. There are different ways of defining the external and internal forces of the active contours; the most popular is GVF (Gradient Vector Flow) which is described in [4].
On a given image $I(x, y)$ an edge map $f(x, y)$ is defined. Starting with $u = \nabla f$ one iterates Eq. 12 to find the equilibrium solution.

$$u_t = \mu \nabla^2 u + \left|\nabla f\right|^2 (u - \nabla f) \qquad (12)$$

The equilibrium solution V is then used to determine the shape of the active contour. This is done by iterating Eq. 13. The right hand side of Eq. 13 is zero for the stationary solution. This solution is typically reached after 120 steps.

$$x_t(s,t) = \alpha x''(s,t) - \beta x''''(s,t) + V \qquad (13)$$

The contour is given as a function of s and t. $s \in [0,1]$ is the parameterisation of the contour curve and t is the time parameter indicating the iteration step. x' is the derivative with respect to s.

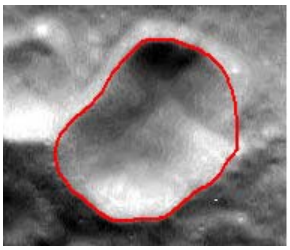

Fig. 3: A sample crater as determined by the active contour method.

The sample crater image shown in Fig. 3 was delivered by the AMIE camera on board of SMART1 satellite. We successfully extrapolated the shapes of craters in the mare and highland region of the Moon. All crater shapes which had more than 150 pixel diameter were extrapolated using the same parameters α, β etc., which determine the convergence of the active contour.

5. EXTRACTION OF STATISTICAL PARAMETERS

To estimate the radial standard deviation σ and the power law coefficient ν, the rim profile as determined by the active contour fitting needs to be equidistantly gridded in the angular direction. The estimation of the statistical parameters is then done by comparing the set of the rim profiles belonging to the same group to the sample sets of shapes with known power law coefficient and known standard deviation.

The quality of the agreement between the retrieved shapes and the sample shapes is characterized by comparing the χ^2_{red} value, the agreement is the better the lower χ^2_{red}.

To compute the χ^2_{red}, we define a rotationally invariant azimuth angle by equidistantly dividing the length of the curve into a given number of cells. We then compute the angles of the normals of two points along the curve which are an angular distance φ apart and then move along the curve an angle Φ further and calculate the normals again. This procedure is repeated for each of the sample curves n times, the agreement of both sample sets is tested with χ^2_{red} [5].
The sample shapes can be compared either to a set of Gaussian circles or to Gaussian spheres, the correlation function is the given by Eq. 9 and Eq. 7 respectively.

When estimating the parameters of the corresponding random Gaussian sphere, one needs to take into account that the extrapolated rim circle corresponds to a cross-section at a given height value of the random sphere, which is not the equator of the random sphere.

6. LIGHT SCATTERING INSIDE CRATERS

We implemented a ray tracing procedure to study the light scattering inside the sample Gaussian shapes. We assumed the Lommel Seeliger scattering law as given in Eq. 14

$$S_{LS} = \frac{\varpi \cdot p(\alpha)}{4\pi} \cdot \frac{1}{Cos(\theta_{in}) + Cos(\theta_{out})} \qquad (14)$$

In this equation, ϖ is the single scattering albedo, $p(\alpha)$ is the single particle phase function and the angles θ_{in} and θ_{out} are the angle of incidence and the angle of emergence respectively.
The irradiance L_{direct} received by a cell with an area A_1 from direct radiation is given by the Eq. 15

$$L_{direct} = \cos(\theta_{in}) \cdot A_1 \qquad (15)$$

We assume a unidirectional incident flux of $1\frac{W}{m^2}$.

As there is no compact mathematical relationship to find out whether a cell is directly illuminated or not, we determined this by tracing a ray from the cell center in the inverse direction of the incident illumination, and determined whether the ray would escape the crater. If this was the case, the cell was considered to be directly illuminated.

Though the local incidence and emergence angles change, the phase angle remains the same for all cells for fixed viewing conditions. We therefore used a constant to approximate the phase function $\varpi \cdot p(\alpha) = const$. This is a multiplicative constant, which varies depending on the angle of emergence and incidence. Varying this constant does not change the spatial scattering distribution; this distribution is only determined by the local angle of incidence.

We did not consider second level scattering, because the effect resulted in a deviation of less then 1% of the emitted radiance values and was found to be much more CPU time consuming.

Using Eq. 14 with the assumptions above, we could determine the radiance emitted by each cell in the viewing direction. To determine, whether the emitted ray could escape the crater, we used the same method as for determining whether or not a cell is illuminated. The results of this study are shown in Fig. 4.. it shows the spatial light distribution inside a sample crater with a diameter-to-depth ratio of 5, $\sigma = 6\%$ and $\nu = 3$. The light enters the crater along the x-axis (red) with an inclination of 45^o and the observer is looking parallel to the incoming light. To generate the plot in Fig. 4 we used $\varpi \cdot p(\alpha) = 0.03$. The maximum value emitted by a cell in this example is $1.6 \cdot 10^{-6}$ Watt, the minimum is zero due to the shadowed regions.

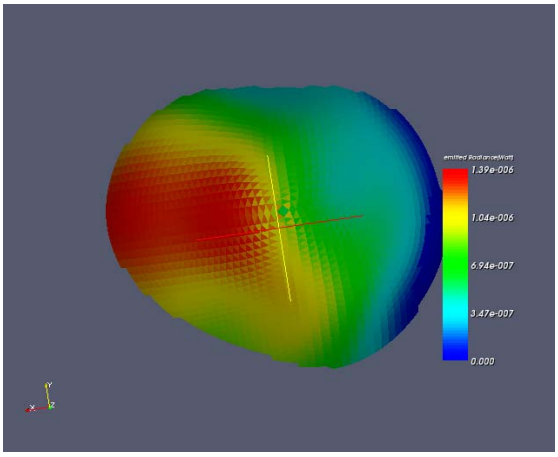

Fig. 4: Colour-coded emitted radiance in the direction of the observer. The maximum values are denoted in red, the minimum values in blue.

7. RESULTS AND DISCUSSION

The two parameter statistical model presented in this paper has the advantage of offering a compact description for a variety of crater shapes. The advantage of the two statistical parameters compared to a fit with Zernike polynomials [7] is the low number of parameters and the direct physical interpretation of them.

Using our method, we studied the crater shapes of the mare and highland regions on the Moon, and found that the radial deviation σ is typically 3 to 5 %, and the power law coefficient ν is approximately 3 to 4. The number of the extrapolated sample crater rims was 24 in this study. We plan to extend this to higher number of sample shapes and to study the statistical parameters of different regions.

The first results suggest that the total integrated brightness of more deformed craters can be up to 5% higher or lower compared to the integrated brightness of a homogenous sphere with the same diameter-to-depth ratio.

8. OUTLOOK

The compact two parameter statistical model is a powerful tool for characterizing the crater shapes as well as the crater rim profiles. Several questions are interesting: Do the statistical parameters depend on the planetary body, the soil material and the angle of impact? How can we qualitatively and quantitatively access this dependence? How much influence does the shape have on the integrated brightness of the crater?

9. ACKNOWLEDGEMENTS

We gratefully acknowledge the support of the German National Academic Foundation, the Muehlfenzl Foundation, and the Physics Faculty of the TU Darmstadt.

10. REFERENCES

[1] C. J. Solomon et al., *Automated compact parametric representation of impact craters*, Int. J. Impact Engineering Vol. 21, No.10, p. 895-904, 1998.

[2] K. Muinonen and J.S.V. Lagerros, *Inversion of shape statistics for small solar systems bodies*, A&A 333, 753-761, 1998

[3] Pike et al., *Size-dependence in the shape of fresh impact craters on the moon* in Eds., Impact and explosion cratering. Pergamon Press, New York, 489-509, 1977

[4] C. Xu, J. L. Prince, *Snakes, Shapes, and Gradient Vector Flow* IEEE Transactions on image processing, Vol. 7, No. 3, March 1998

[5] Muinonen, K. (2006). *Inversion of small-particle silhouettes for Gaussian-sphere parameters*, Proceedings of the 9th Conference on Electromagnetic and Light Scattering by Nonspherical Particles: Theory, Measurements, and Applications, St. Petersburg, Russia, June 5-9, 2006, 4 pp., in press.

[6] A.P. Ingersol et al., *Stability of Polar Frosts in Spherical Bowl-Shaped Craters of Moon, Mercury, and Mars*, Icarus 100, 40-47 1992

[7] D.Wallis, C.J. Solomon, and N. McBride., *Modelling radially symmetric impact craters with orthogonal functions,* Int. J. Impact Engineering, 2000

[8] L. Lamberg et al, *Spectral estimation of Gaussian random circles and spheres*, Journal of Computational and Applied Mathematics 136 (2001) 109–121